PHYSICAL AND MECHANICAL PROPERTIES OF THE NANOCOMPOSITE AND COMBINED Ti-N-Si /WC-Co-Cr/ AND Ti-N-Si/(CR₃C₂)₇₅-(NiCr)₂₅ COATINGS

A.D. Pogrebnjak[1,2], M.V. Il'yashenko[1], M.V. Kaverin[1,2], A.P. Shypylenko[1], A.V. Pshyk[1], V.M. Beresnev[3], G.V. Kirik[4], N.K. Erdybayeva[5], N.A. Makhmudov[6], O.V. Kolisnichenko[7], Yu.N. Tyurin[7], A.P. Shpak[8]

[1] Sumy Institute for Surface Modification,
    P.O. Box 163, 40030, Sumy, Ukraine
    E-mail: apogrebnjak@simp.sumy.ua

[2] Sumy State University,
    2, Rimsky-Korsakov Str., 40007, Sumy, Ukraine

[3] Science Center for Physics and Technology,
    6, Svobody Sq., 61022, Kharkov, Ukraine

[4] Concern "Ukrrosmetal",
    6, Kursky Ave, 40020, Sumy, Ukraine

[5] East-Kazakhstan State Technical University,
    69, Protazanov Str., 070004, Ust-Kamenogorsk, Kazakhstan

[6] Samarkand State University,
    15, University Boulevard, 140104, Samarkand, Uzbekistan

[7] E.O. Paton Welding Institute, NAS of Ukraine,
    11, Bozhenko Str., 03680, Kiev, Ukraine

[8] G.V. Kurdyumov Institute of Metal Physics, NAS of Ukraine,
    36, Vernadsky Boulevard, 03680, Kiev, Ukraine

Two types of the combined nanocomposite coatings (Ti-N-Si /WC-Co-Cr and Ti-N-Si/ (Cr₃C₂Ni)₇₅-(NiCr)₂₅) of 160-320 μm thickness were produced using two deposition techniques: the cumulative-detonation and the vacuum-arc deposition with the high-frequency discharge. This gives the possibility (using the combined coatings) to restore the size of worn areas of the tools and demonstrate the high corrosion and wear resistance, to increase the hardness, modulus of elasticity, and plasticity index. Composition of the top coating varied from Ti = 60 at.%, N ≈ 30 at.%, and Si = 10 at.% to Ti = 75 at.%, N ≈ 20 at.%, and Si = 5 at.%. In the first series of coatings the following phases were obtained: (Ti;Si) and TiN in thin top coating and WC and W₂C in thick bottom coating. The second series gives (Ti;Si)N and TiN in top coating; Cr₃Ni₂ and pure Cr in bottom coating; and small amount of Ti₁₉O₁₇ in the transition region between thin and thick coatings. For the first series the grain size achieved 25 nm at the hardness of 38 GPa. For the second series the grain size was 15 nm at the hardness of 42 GPa ± 4 GPa. It is shown that the corrosion resistance in salt solution and acid media increases with the wear decrease as a result of the cylinder friction over the surface of combined coating.

1. INTRODUCTION

Nanocomposites as a class of nanomaterials are characterized by heterogeneous structure of formations in the material with practically non-interacting phases of mean sizes in the interval 5-35 nm [1-3]. As a rule, the amorphous matrix and inclusions of nanocrystalline phase are such structure elements.

Here the amorphous component is best agreed with the nanocrystalline surface and provides good cohesion that leads to the substantial strength increase, and high mechanical properties of such composite are provided by the small size of the second phase in combination with a good strength of the intergrain boundaries. Currently all nanocomposite materials are divided into three classes in terms of the quantity of hardness: hard nanocomposites with the hardness from 20 to 40 GPa, superhard nanocomposites with the hardness in the range of 40-80 GPa, and ultrahard nanocomposite coatings with very high hardness (higher than 80 GPa) [3-4].

Moreover, to solve a number of problems in chemical, machine-building and other fields, it is necessary to restore the element size (which already operate in production) besides solving the direct protection functions of the coatings. Therefore to obtain the product size, a thick enough coating, which has higher physical and mechanical properties than the base metal, is deposited. Alloys (powders) from Ni-Cr-Mo [5], hard alloys WC-Co-Cr [8], Cr_3C_2-Ni, oxide ceramics Al_2O_3, $Al_2O_3 + Cr_2O_3$ [5, 7] are usually used in such coatings. Thus, if make the coating combination, which consists of at least two coating layers, for example, of the hard alloy based on WC-Co-Cr with the thickness higher than 100 μm (by the cumulative-detonation or detonation method), and then deposit the top thin nanocomposite coating of the thickness of some μm, for example, from Ti-Si-N, which has higher physical and mechanical characteristics in comparison with thick coatings, as a result we obtained the combined nanocomposite coating with high physical and mechanical properties, such as the hardness H, the modulus of elasticity E, the elastic restitution W_e, the material resistance to plastic deformation H/E, and the plasticity index H_2/E_2 [3].

Thus, the aim of the present work was to create the nanocomposite coatings based on Ti-Si-N and the combined nanocomposite coatings based on Ti-Si-N/ WC-Co-Cr and Ti-Si-N/Cr_3C_2-NiCr with high hardness, and to investigate their physical and chemical and mechanical properties.

2. DETAILS OF THE EXPERIMENT

Coatings were deposited on the polished steel samples with the thickness of 4 mm and 20 mm by the vacuum-arc source with the high-frequency (HF) discharge. The alloyed sintered Ti cathode with Si content of 5-10 at% was used in the plant Bulat 3T with the vacuum $5 \cdot 10^{-5}$ Pa, the cathode current is 100 A. The coating was deposited on another series of the cylinder steel samples 3 (0,3% C) with the diameter of 20 mm and the thickness of 4-5 mm using the cumulative-detonation plant "CDS-1" [17] with the following parameters: the distance from the nozzle section is 65 mm, the conveying

speed is 14 mm/s, the number of transitions is 5, the pulse-repetition frequency is f = 12 Hz (for WC-Co-Cr). Thickness of the thick coating was 160-320 μm. After coating deposition the surface layer was fused by the plasma jet (without powder) with the eroding W electrode. Thickness of the fused layer was 45-60 μm. Then the thin Ti-Si-N coating of the thickness of 3 μm was deposited on the thick coating in the same plant Bulat 3T.

For $(Cr_3C_2)_{75}(NiCr)_{25}$ coating the main fraction of the powder is 37,8 μm. The distance from the nozzle section is 70 mm, the conveying speed is 4 mm/s, the number of transitions is 4, the pulse-repetition frequency is 10 Hz and the capacity of the capacitor bank is C = 200 μF, the voltage on the capacitor bank is 3,2 kV.

To analyze the element composition the following methods were used: the Rutherford backscattering of $^4He^+$ ions with the energy of 1,76 MeV, the scanning electron microscopy on the plant REMMA-103M (Selmi, Ukraine), the X-ray diffraction on the plants DRON-3 and Advantage-8 (USA).

Measurements of the hardness and the modulus of elasticity were performed using the nanohardometer Nanoindenter G-200, MTS System Corporation, Oak Ridge TN (USA) with the Berkovich pyramid. The modulus of elasticity was determined using the curves "load-reload" by the Oliver-Pharr method [15].

3. RESULTS AND DISCUSSION

The regime of detonation combustion of the fuel mixtures (and gases) is realized in the cumulative-detonation device.
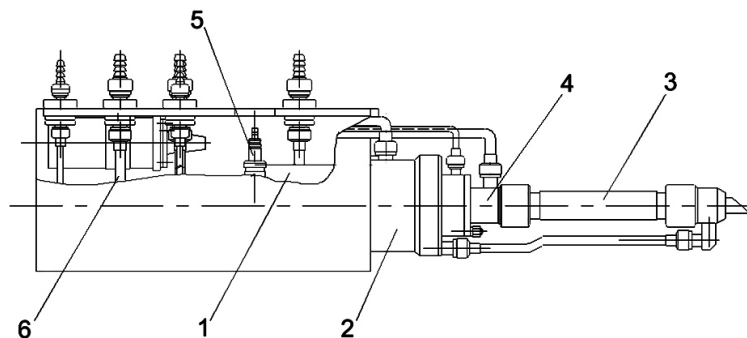

Fig. 1 − Cumulative-detonation gun (CDS-1)

Device in Fig. 1 consists of the detonation chamber 1, where the detonation regime of combustion of the fuel gas mixture is realized. Moreover, the device contains the cumulative-detonation chamber 2, which operates with the fuel mixtures of any concentration, that allows to form the high-speed gas jet with the nitrogen and carbon surplus. The cylindrical nozzle 3 is destined for heating and acceleration of powder materials. It is made of the copper tubes and can have any configuration of the cross-section and the output diameter from 10 mm to 33 mm. In addition, CDS-1 has unit 4 for the input and gas cutoff of the gas-powder mixture, the motor spark-plug 5 for the initiation of the detonation regime of combustion, and the pipeline system 6 for the input of the fuel gas mixture components. The main operation difference between the cumulative-detonation device and the detonation one is in the following: in the first device the energy summation of the

detonation combustion products of the fuel mixtures from two chambers is realized. The energy cumulation allows to form the high-speed working gas flow, which has some shock waves, that provides their effective interaction with the powder material. This provides the efficient use of the fuel and gas mixture energy.

Velocity and temperature of the combustion products depend only on the combustion regime in each chamber.

Nozzles for the cumulative-detonation device operate no less than 1000 hours; the high frequency of combustion initiation (15-30 Hz) in CDS-1 provides the feasibility of the quasi-continuous coating deposition technique.

In Fig. 2 we present the image of the surface area of the nanocomposite combined Ti-Si-N/WC-Co-Cr/ChS-4Z (43% Ni) coating.
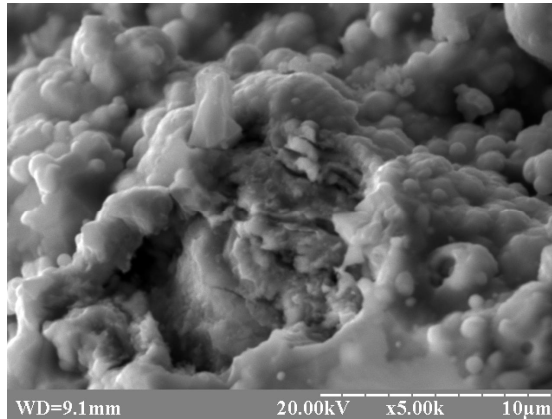

WD=9.1mm   20.00kV   x5.00k   10μm

Fig. 2 – *Image of the surface area of the nanocomposite combined Ti-Si-$N/(Cr_3C_3$-$Ni)_{75}$-$(NiCr)_{35}$ coating*

Thin coating is obtained using the plasma-detonation technique. Mean size of the roughness is 14-22 μm (after fusion and deposition of the thin coating by the vacuum-arc source). In Fig. 3 we present the image of the X-ray energy-dispersive spectrum, which gives the following concentrations: N ~ 7,2-7,52 at%, Si ~ 0,57 at%, Ti ~ 76,70 at% and Fe ~ 0,7 at%; Ni, Cr, Fe from the thick coating has small dispersion.

In Fig. 4a we show the results of the Rutherford backscattering analysis for the thick WC-Co-Cr coating (without thin Ti-Si-N coating), and the results obtained from the combined coating are presented in Fig. 4b.

As seen from the calculation results (element distribution) using the standard program [5], the concentration estimates show that N = 30 at%, Si ≈ 5-6 at% and Ti ≈ 64-63 at%. It is difficult to estimate the element concentration from the energy spectrum obtained on the thick coating due to the high roughness of the coating surface prepared by the plasma-detonation method.

Results of the X-ray phase analysis obtained for the combined nanocomposite coating showed (see Fig. 5) that in the composition of two-layer structure the following phases are formed: (Ti;Si)N, TiN in thin nanocomposite film; WC, W_2C. The last phases were formed in the thick coating. For the hardness measurements the special samples were prepared: their surface was firstly planished and then polished. After deposition of the thick WC-Co-Cr

coating the thickness of the formed layer was 120 μm, and as a result of the polishing its thickness increased to 80-90 μm. Ti-Si-N film of the thickness of about 3 μm was deposited on the polished surface. It was found during the investigations that the hardness of different surface regions substantially changes from 29 ± 4 GPa to 32 ± 6 GPa. It is probably connected with the following: the coating obtained by the plasma-detonation method is inhomogeneous over the surface due to the spread in hardness values in the thick coating from 17,3 GPa to 11,5 GPa. Possibly, this relation of the hardness values keeps after deposition of the thin Ti-Si-N coating. In this case the modulus of elasticity has the same non-ordinary behavior, namely, with the load increase it increases and becomes saturated at the indenting depth of indenter ≥ 200 nm.

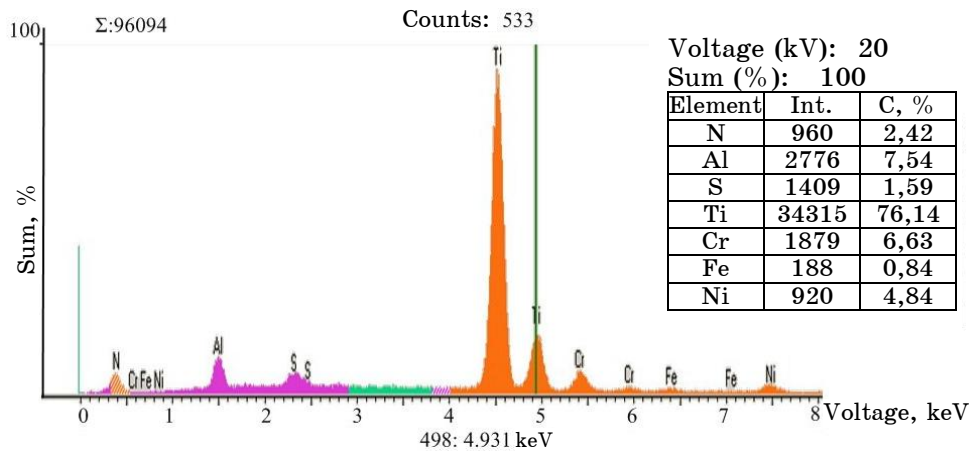| Element	Int.	C, %
N	960	2,42
Al	2776	7,54
S	1409	1,59
Ti	34315	76,14
Cr	1879	6,63
Fe	188	0,84
Ni	920	4,84

Voltage (kV): 20
Sum (%): 100

Fig. 3 − Element composition obtained using the X-ray energy-dispersive analysis from the surface area of the combined coating

Hardness of the thin coating deposited on the polished surface ST-45 has the maximum value 48 GPa, and the mean value $H_m = 45$ GPa. As seen from the results, the spread in hardness values is substantially smaller than in the combined coating.

In Fig. 6 we present the dependences "load-reload" for different indenting depths of indenter. As seen from these dependences and performed calculations in accordance with the Oliver and Pharr method [15], the hardness of Ti-Si-N coatings deposited on the thick $(Cr_3C_2)_{75}$-$(NiCr)_{25}$ coating is 37 ± 4 GPa at the modulus of elasticity $E = 483$ GPa.

In Fig. 7 we present the fragments of the diffraction patterns obtained on the nanocomposite combined Ti-Si-N/$(Cr_3C_2)_{75}$-$(NiCr)_{25}$ coating. Results of the diffraction analysis and calculations for the coating structure parameters are represented in Table 1.

In the coating the main phases are Cr_3Ni_2 (the thick bottom coating) and (Ti;Si)N and TiN (the top coating layer). Besides, there are additional phases of pure Cr; and titanium oxide Ti_9O_{17} is also present in a small concentration on the interphase boundary.
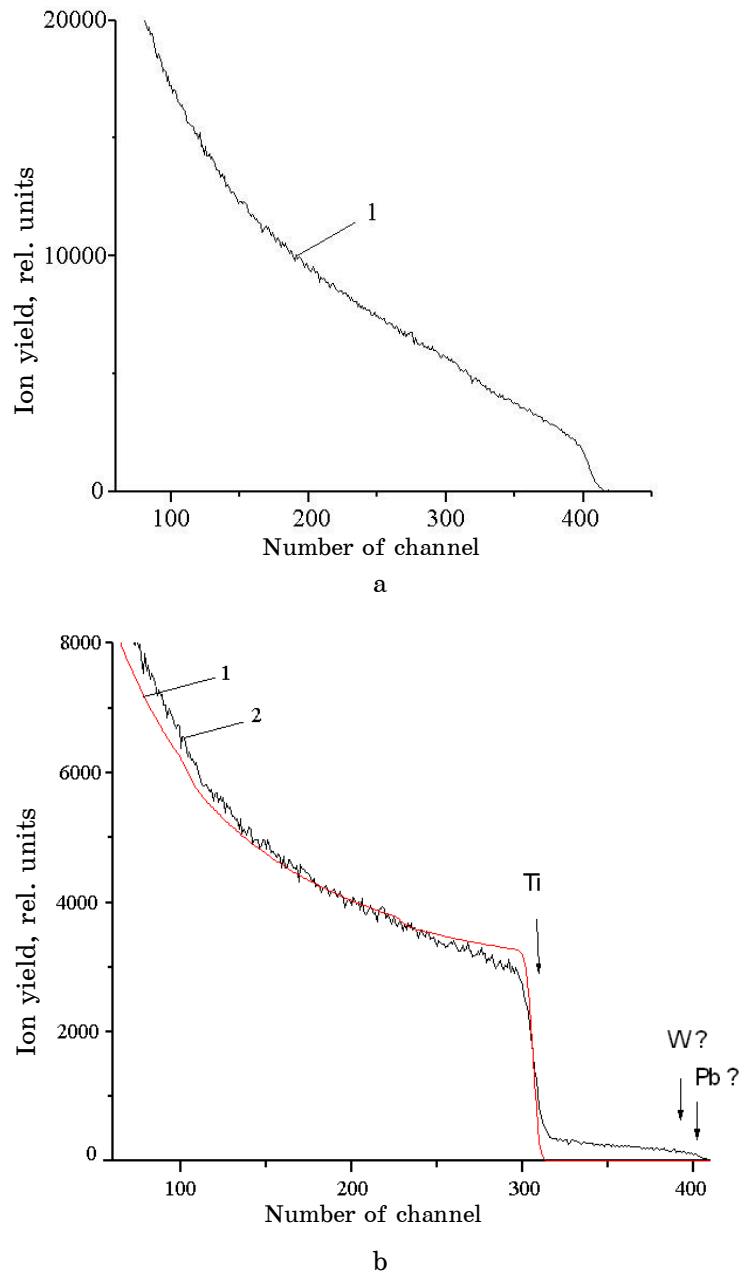
Fig. 4 − *Energy spectrum of the Rutherford ion backscattering: on the thick WC-Co-Cr coating (1 is the experimental spectrum of WC-Co-Cr) (a); obtained from the thin top Ti-Si-N/WC-Co-Cr coating (1 is the simulated spectrum; 2 is the experimental spectrum of Ti-Si) (b)*
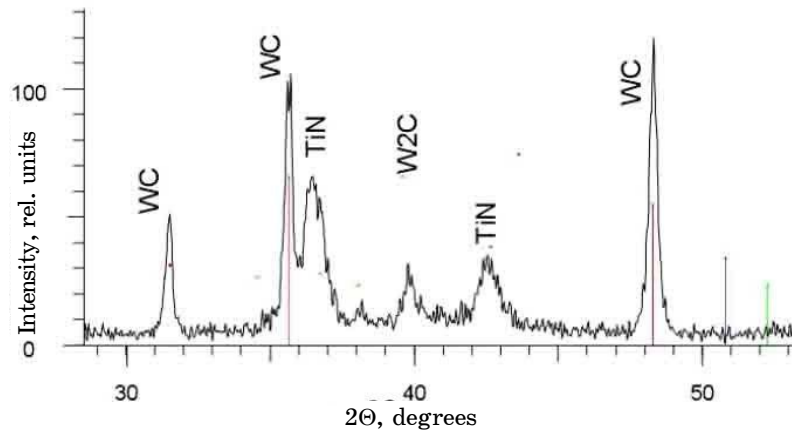
Fig. 5 *− Fragments of the diffraction pattern obtained from the surface region of the nanocomposite combined Ti-Si-N/WC-Co-Cr coating deposited on the ChS-42 steel substrate*
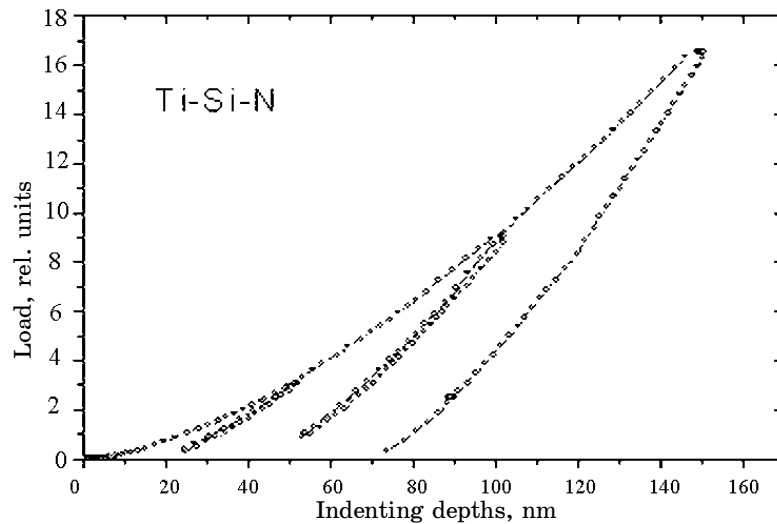

Fig. 6 *− Dependences "load-reload" for different indenting depths of the Berkovich indenter in the nanocomposite Ti-Si-N/(Cr$_3$C$_2$)$_{75}$(NiCr)$_{25}$ coating*

In view of the low Si content the superposition of diffraction peaks of (Ti;Si)N and TiN phases occurs, and (Ti;Si)N is the solid solution based on TiN (Si intrusion). These phases are well separated on the angles 72-73°.

In Fig. 8 we present regions of the thick bottom (Cr$_3$C)$_{75}$-(NiCr)$_{25}$ coating and distribution of the X-radiation intensities of the base elements. The main composition of this coating is nickel (Ni ~ 36 at%) and chrome (Cr ~ 64 at%), C, O and Si are also present.
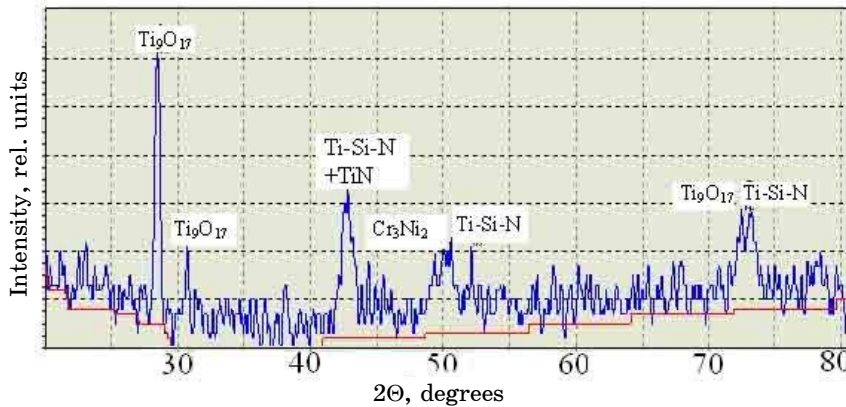
Fig. 7 − *Part of the diffraction pattern of the nanocomposite combined Ti-Si-N/ (Cr₃C₂)₇₅-(NiCr)₂₅ coating*

Table 1 − *Calculation results of the coating parameters and structure*

No/ Par.	Angle	Square	Intensity	Half-width	Interplanar spacing	% Max.	Phase	hkl
1	28,437	8,511	37	0,4512	3,6416	100,00	Ti_9O_{17}	106 004
2	30,648	3,083	13	0,4518	3,3845	36,84	Ti_9O_{17}	0210 123
3	42,771	10,885	20	1,0490	2,4530	65,79	Ti-Si-N TiN	111 111
4	49,332	13,862	13	1,9890	2,1433	34,21	Cr_3Ni_2 Ti-Si-N	321 200
5	49,993	17,418	15	2,2322	2,1168	39,47	TiN Ti_9O_{17}	200 1223 110
6	50,533	6,528	12	1,0335	2,0956	44,74	Cr_3Ni_2	330
7	52,134	2,782	15	0,3553	2,0355	39,47	Cr_3Ni_2 Cr Ni	202 110 111
8	72,500	18,056	18	1,8950	1,5127	47,37	Ti_9O_{17} Ti-Si-N	3130 220
9	73,040	11,106	13	1,5950	1,5030	52,63	TiN	220

Since the thin top coating has very small thickness, it is difficult to extract it on the cross-sections due to the large width of the detonation coating. There are areas in the coating corresponding to the pure nickel and chrome. In the nickel matrix (white region) there is substantial amount of chrome inclusions (grains): fine (< 1 μm), middle (4-5 μm) and coarse (15-20 μm). White region is rich in Ni (up to 90 at%), and grey region is rich in Cr (up to 92 at%). Due to the small thickness of Ti-Si-N layer in these experiments we could not determine using microanalysis the composition and thickness, and also because of the restriction of the element composition detection (nitrogen, carbon, oxygen). However, while obtaining the oblique cross-sections at the angle of 7°, we could reveal the element composition of the thin Ti-Si-N coating and of the thick bottom $(Cr_3-C_2)_{75}$-$(NiCr)_{25}$ coating taking 10-12 points

of the oblique cross-section and using another scanning microscope with better energy resolution.
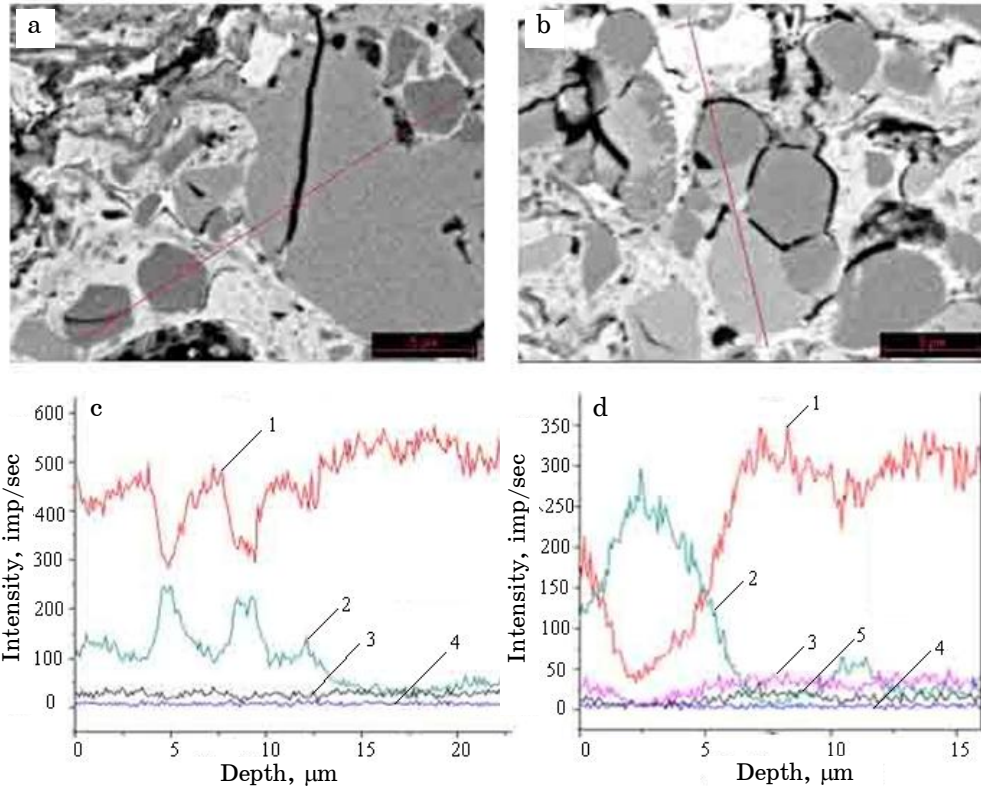

Fig. 8 − *Parts of the cross-sections of the combined coatings obtained by the scanning electron microscopy: lines of the element analysis obtained by the EMF (1 − Cr, 2 − Ni, 3 − C, 4 − Fe) (a, b); the element distribution over the depth of the combined Ti-Si-N(Cr₃C₂-Ni)-(NiCr)₂₅ coating on the regions shown in Fig. 8a, b (1 − Cr, 2 − Ni, 3 − C, 4 − Fe, 5 − O) (c, d)*

4. CONCLUSIONS

Nanocomposite combined Ti-Si-N/WC-Co-Cr and Ti-Si-N/(Cr$_3$C$_2$)$_{75}$(NiCr)$_{25}$ coatings with the thickness > 100 μm are obtained and investigated. Found that the grain size of the thin coatings formed by (Ti;Si)N and TiN phases at the hardness of 38 GPa was ≈ 25 nm for the first series of the samples. For the second series the grain size was lesser (about 15 nm) at the coating hardness of 42-44 GPa and the same composition of (Ti;Si)N and TiN phases. Si and N concentrations varied from 10 at% (Ti) to 5 at% (Si) and from 30 at% to 20 at% (for N).

We have also found the substantial increase in the wear resistance at the cylinder abrasion on the sample plane and in the corrosion resistance at the rise of other mechanical characteristics.

REFERENCES

1. H. Gleiter, *Acta Mater.* **48, 1** (2000).
2. S. Veprek, M. Veprek-Heijman, P. Karvankova, S. Prochazka, *Thin Solid Films* **476, 1** (2005).
3. J. Musil, *Physical and mechanical properties of hard nanocomposite films prepared by reactive magnetron sputtering* (New York: Nanostructured Hard Coatings: 2005).
4. A.D. Pogrebnjak, A.P. Shpak, N.A. Azarenkov, V.M. Beresnev, *Phys.-Usp.* **52 No1, 29** (2009).
5. K.K. Kadyrzhanov, F.F. Komarov, A.D. Pogrebnjak, *Ionno-luchevaya i ionno-plazmennaya modifikatsiya materialov* (M: MGU: 2005).
6. A. Gavaleiro, J.T. De Hosson, *Nanostructured Coating* (Berlin: Springer-Verlag: 2006).
7. R.A. Andrievski, A.M. Glezer, *Phys. Usp.* **52 No4, 315** (2009).
8. N.A. Azarenkov, V.M. Beresnev, A.D. Pogrebnjak, *Struktura i svoistva zaschitnyh pokrytiy i modifitsirovannyh sloev*, 560 (Kharkov: KhNU: 2007).
9. V.M. Beresnev, A.D. Pogrebnjak, N.A. Azarenkov, G.V. Kirik, V.I. Farenik, V.V. Ponaryadov, *Uspehi fiz. met.* **3**, 171 (2007).
10. G.P. Glazunov, A.A. Andreev, V.M. Shulaev, *Kharkovskaya nanotekhnologicheskaya assambleya* **1**, 187 (Kharkov: NNTs KhFTI: 2006).
11. E.A. Levashov, D.V. Shtansky, *Russ. Chem. Rev.* **76 No5, 463** (2007).
12. R.F. Zhang, S. Veprek, A.S. Argon, *Phys. Rev. B* **79, 245436** (2009).
13. S. Veprek, A.S. Argon, R.F. Zhang, *Phil. Mag. Lett.* **12, 955** (2007).
14. J. Musil, P. Barozh, P. Zeman, *Plasma Surfaces Engineering and its Practical Applications* (Research Signpost Publisher: 2007).
15. S.N. Dub, N.V. Novikov, *Sverhtverdye materialy* **6**, 16 (2004).
16. A.D. Pogrebnjak, Yu.A. Kravchenko, *Poverhnost'* No11, 74 (2006).
17. A.D. Pogrebnyak, Yu.N. Tyurin, *Phys.-Usp.* **48, 487** (2005).